

## FRP ANCHORS: RECENT ADVANCES IN RESEARCH AND UNDERSTANDING

S.T. Smith  
 Department of Civil Engineering  
 The University of Hong Kong, China.  
 Email: stsmith@hku.hk

### ABSTRACT

The effectiveness of strengthening reinforced concrete (RC) members with externally bonded fibre-reinforced polymer (FRP) composites may be compromised by premature debonding failure of the FRP prior to its ultimate strength being reached. An anchorage system which can delay or even eliminate debonding failure is therefore of most importance in order to improve the efficiency, reliability and safety of FRP strengthening. Anchors made from FRP (known as *FRP anchors*) are an attractive form of anchorage as they are non-corrosive and can be applied to a wide variety of structural elements. Surprisingly, little research has been undertaken on the characterisation of such anchors though and it is this limitation in knowledge which is prohibiting their rational design and wide-scale use. This paper in turn presents recent advances in research and understanding of the strength and behaviour of FRP anchors. In addition, future research needs are also identified.

### KEYWORDS

Anchors, bond, FRP, IC debonding, joints, pullout, shear.

### INTRODUCTION

Numerous experimental investigations to date have established that reinforced concrete (RC) members can be strengthened with externally bonded fibre-reinforced polymer (FRP) composites (e.g. ACI 2007, Hollaway and Teng 2008). A commonly reported failure mode is debonding of the FRP strengthening (herein *FRP plate*) from the concrete substrate with debonding initiating near the end of the FRP plate or at intermediate cracks in the member (Oehlers and Seracino 2004, Hollaway and Teng 2008). Such debonding failures are generally sudden and are hence undesirable. In order to halt the propagation of debonding cracks, FRP anchors can be applied to the FRP plate. The FRP anchors developed to date by researchers have been handmade in the laboratory and are essentially rolled carbon or glass fibre sheets. Handmade anchors may also be formed from bundles of fibres. Also, commercially made FRP anchors are available on the market however they are not considered herein. In terms of the components of a FRP anchor, one end of the anchor (i.e. the dowel portion) may be impregnated with epoxy (e.g. Figures 1a and 1b) or not (Figures 1c and 1d). It is this end which is inserted into predrilled epoxy filled holes in the concrete substrate. The other end of the anchor consists of dry fibres (i.e. anchor fan portion) which is threaded through the FRP plate and splayed then epoxied onto the FRP plate surface in order to disperse stress concentrations.



(a) Impregnated carbon FRP anchor

(b) Impregnated glass FRP anchor

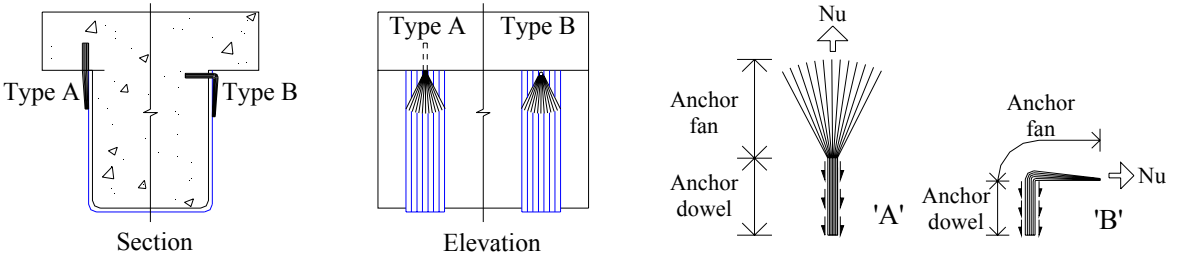
(c) Unimpregnated (dry) carbon FRP anchor

(d) Unimpregnated (dry) glass FRP anchor

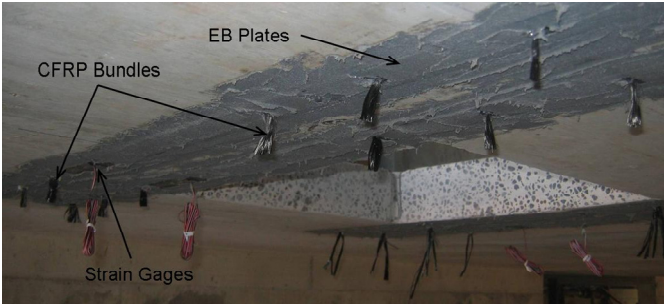
Figure 1. Carbon and glass FRP anchors

It is the orientation of the installed FRP anchor which determines the nature of the forces it will be subjected to. To illustrate this concept, Figure 2 shows FRP anchors installed to secure the free ends of FRP U-jackets used for shear strengthening of a RC T-beam. As a result, the FRP anchor can be subjected to predominantly pullout

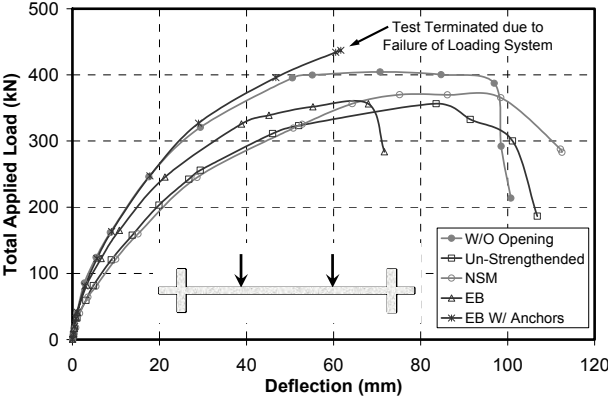
forces (anchor Type A in Figure 2) or shear forces (anchor Type B in Figure 2: tensile forces will also be present). Various structural shapes and materials such as RC beams (e.g. Oh and Sim 2004, Orton et al. 2008), RC slabs (e.g. Lam and Teng 2001, Seliem et al. 2008) and masonry walls (e.g. Tan and Patoary 2004) have been strengthened with FRP plates and installed with FRP anchors of various orientations. Figure 3a shows one of Seliem et al.'s (2008) slab tests in which FRP strengthening has been applied either side of a cutout made to an existing RC slab. FRP anchors have been inserted through the FRP plates however the fan fibres have not yet been splayed and epoxied onto the FRP plates beneath. For this case, the FRP anchors are subjected to a predominantly shearing action. Figure 3b shows the corresponding load-deflection responses.



(a) FRP anchor types and applications (b) FRP anchor types and dowel stress distribution  
 Figure 2. FRP anchors in U-jacket shear strengthening



(a) Installation of FRP anchors



(b) Load-deflection responses of unanchored and anchored EB FRP and NSM FRP  
 Figure 3. Field application and structural response  
 {EB = externally bonded, NSM = near surface mounted}

Research on the strength and behaviour of FRP anchors in isolation has however been much more limited and such research has been predominantly experimental. Studies to date have reported the pullout strength and behaviour (Özdemir 2005, Kim and Smith 2009a, Ozbakkaloglu and Saatcioglu 2009) as well as the shear strength and behaviour (e.g. Aiello et al. 2004, Smith and Kim 2008, Kim and Smith 2009b) of FRP anchors. As a result of such limited research, there is very limited design guidance available for both handmade and commercially available FRP anchors. This paper in turn presents a snapshot of some of the latest research developments pertaining to the characterisation of FRP anchors. More specifically, research related to the strength and behaviour of FRP anchors under pullout forces and shear forces is presented in addition to future research needs.

## PULLOUT STRENGTH AND BEHAVIOUR OF FRP ANCHORS

Anchors (whether metal or FRP) are defined by load transfer mechanism (i.e. mechanical interlock, friction, chemical bond, or various combinations) (Eligehausen et al. 2006). Anchors can also be defined by their method of installation (i.e. cast-in-place, drilled-in or pneumatically installed) (Eligehausen et al. 2006). FRP anchors are drilled in anchors with a chemical bond load transfer mechanism. Examples of adhesive anchors are capsule anchors and injection systems and FRP anchors resemble the latter. Adhesive anchors transfer the load from the anchor, through the adhesive, then into the concrete along the entire bond surface area (Cook et al. 1998) with typical failure modes for adhesive anchors shown schematically in Figure 4. At shallow embedment depths ( $h_{ef} = 3d$  to  $5d$ , where  $d$  is the anchor diameter), concrete cone failure commonly occurs (Figure 4a) and the slope of the cone surface with respect to the top surface of the concrete is approximately  $35^\circ$  (Eligehausen et al. 2006). For greater embedment depths the failure mode usually changes to a combined failure mode of concrete cone and bond failure. The bond failure can be in the adhesive-to-concrete interface, anchor-to-adhesive interface or mixed interface (Figure 4b). Finally, the anchor can also fail by fracture or rupture (Figure 4c).

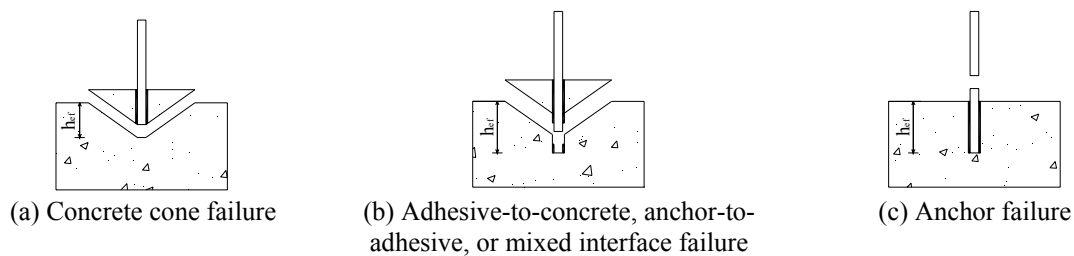


Figure 4. Typical adhesive anchor failure modes

### Experimental Behaviour

Tests on the pull-out strength and behaviour of handmade FRP anchors in uncracked concrete have been reported by Özdemir (2005), Kim and Smith (2009a) and Ozbakkaloglu and Saatcioglu (2009). The main parameters investigated were the anchor diameter, anchor embedment depth and concrete compressive strength. Kim and Smith (2009a) observed four different failure modes in their tests, namely, (i) concrete cone failure, (ii) combined failure (cone + bond), (iii) FRP rupture failure, and (iv) interlaminar bond failure within the FRP. Figure 5 provides a summary of each of these failure modes in addition to the combined failure mode of a threaded metal rod. The failure modes are consistent with those observed on existing tests on metal anchors as shown schematically in Figure 4. In the case of anchor rupture failure, Kim and Smith (2009a) have shown handmade FRP anchors to possess a tensile strength as low as 65 % of the strength of flat FRP tensile coupons. In other studies, Özdemir's (2005) anchors failed by rupture, concrete cone failure and combined concrete cone failure and bond failure between the FRP anchor and hole face. The majority of Ozbakkaloglu and Saatcioglu's (2009) anchors failed by combined cone and bond failure while some also failed by rupture. On the whole, the quality of anchor construction was noted to affect the results and it was hypothesised that mass manufactured anchors should have improved quality thus leading to higher strengths with less scatter.

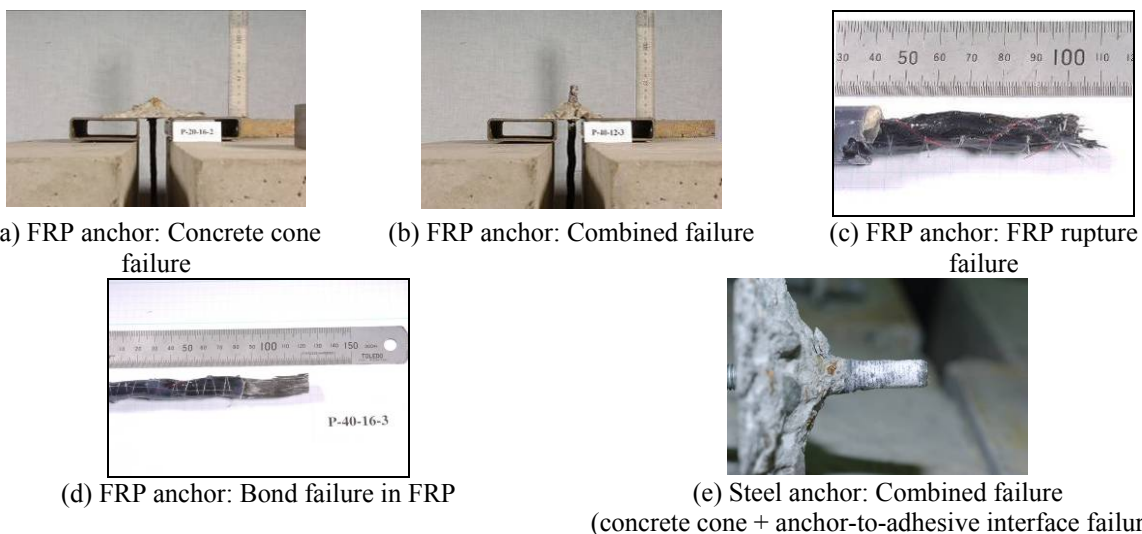


Figure 5. Pullout failure modes of Kim and Smith (2009a)

Load versus concrete surface displacement responses for FRP anchors under tensile load in uncracked concrete are shown in Figure 6 (Kim and Smith 2009a). Pullout strengths equivalent to threaded metal rods of equal diameter were achieved.

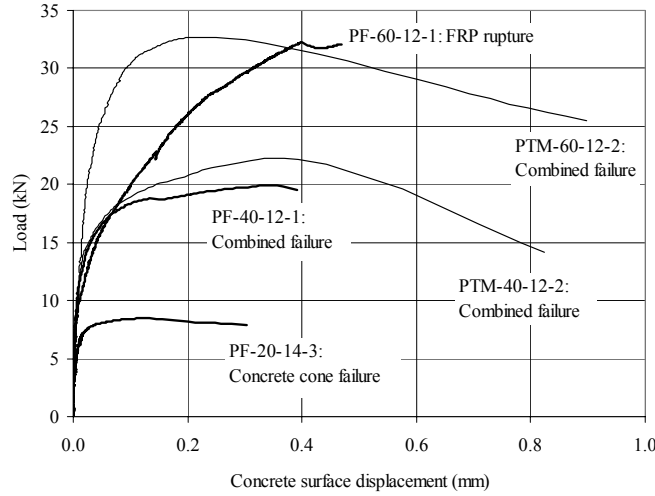


Figure 6. Load versus concrete surface displacement response (PF = FRP anchors, PTM = threaded rods)

### Analytical Modelling

Kim and Smith (2009a) assembled a database of eighty-four tests on FRP-anchors under tensile load control. The results were organised into three failure modes, namely (i) concrete cone failure (30 data-points), (ii) combined failure (46 data-points) and (iii) anchor rupture failure (8 data-points). The ranges of test parameters were  $17.5 \text{ mm} \leq h_{ef} \leq 100.0 \text{ mm}$ ,  $10.4 \text{ MPa} \leq f'_c \leq 60.0 \text{ MPa}$ , and  $11.8 \text{ mm} \leq d_o \leq 20.0 \text{ mm}$ . Kim and Smith (2009c) in turn proposed a set of models to describe the different failure modes. Given the similarity between traditional metal anchor and FRP anchor behaviour in failure mode under tensile forces, existing models originally developed for metal anchors were re-calibrated with the FRP anchor test database. Best fit models as well as design models were proposed with the design versions given as follows;

$$N_u = \min(N_{cc}, N_{cb}, N_{ar}) \quad (1a)$$

$$N_{cc} = 9.68h_{ef}^{1.5} \sqrt{f'_c} \quad (\text{cone failure}) \quad (1b)$$

$$N_{cb} = 4.62\pi d_o h_{ef} \quad (f'_c < 20 \text{ MPa}) \quad (\text{combined failure}) \quad (1c)$$

$$N_{cb} = 9.07\pi d_o h_{ef} \quad (f'_c \geq 20 \text{ MPa}) \quad (\text{combined failure}) \quad (1d)$$

$$N_{ar} = 0.59w_{frp}t_{frp}f_{frp} \quad (\text{anchor failure}) \quad (1e)$$

where the pullout resistance of a single FRP anchor is  $N_u$ , while  $h_{ef}$  is the effective embedment depth of the anchor (mm),  $f'_c$  the concrete cylinder compressive strength (MPa),  $d_o$  the diameter of the anchor hole (mm),  $w_{frp}$  and  $t_{frp}$  the width (mm) and thickness (mm) respectively of the fibre sheet used in construction of the FRP anchor, and  $f_{frp}$  the tensile rupture strength of a flat FRP coupon (MPa). The performances of the best-fit and design models are shown in Figures 7a and 7b respectively.

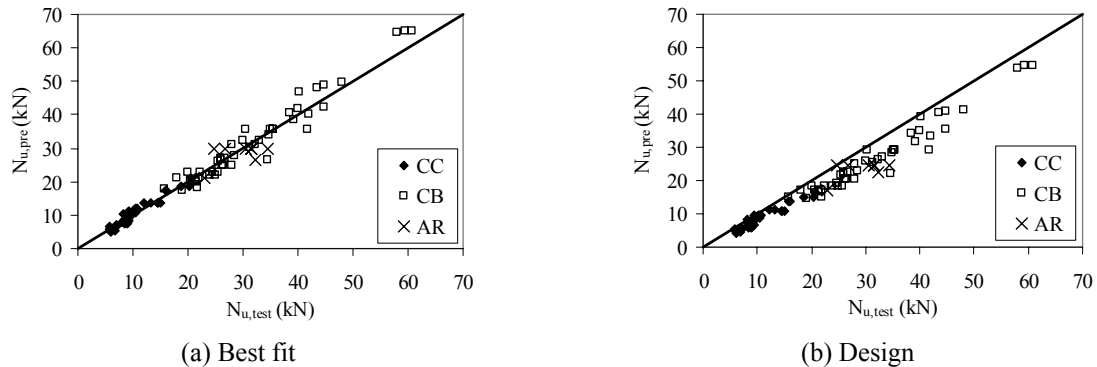


Figure 7. Predicted versus test results  
 {CC = Concrete Cone Failure, CB = Combined (Cone-Bond) Failure, AR = Anchor Rupture Failure}

## SHEAR STRENGTH AND BEHAVIOUR OF FRP ANCHORS

Figure 8 sets the context of the FRP anchor shear research which has been undertaken to date by the author and his research group to date. In this figure, a RC beam is shown which has been strengthened in flexure with a tension face FRP plate. In addition, regularly spaced FRP anchors have been installed. As this beam is loaded, cracks in the beam develop in addition to debonding cracks between the FRP and the concrete substrate at the base of these cracks (especially for slabs and shallow beams) in the region of greatest moment. The debonding cracks eventually become unstable with increased load and propagate to the nearer plate end. This mode of failure is commonly referred to as intermediate crack induced debonding or simply IC debonding (Teng et al. 2003). The FRP anchors can therefore be used to stop the propagation of such debonding cracks in the IC debonding mode. An additional failure mode with which the anchors can be effective is in the prevention of the debonding cracks which initiate in the vicinity of the plate end (i.e. plate end debonding: Oehlers and Seracino 2004, Smith and Teng 2002) which then propagate towards the midspan region. As the position of cracking and debonding failure mode may not be known in advance (e.g. as for virgin members) the anchors may be uniformly spaced as shown in Figure 8a. Upon application of load, cracks can develop away from an anchor (e.g. anchor A in Figure 8a) or much closer to an anchor (e.g. anchor B in Figure 8b). The debonding resistance of the FRP plate between two cracks (with anchor) can in turn be represented by the idealized joint shown in Figure 8b (Teng et al. 2006). The corresponding theoretical elastic interfacial shear stress distribution is given in Figure 8c.

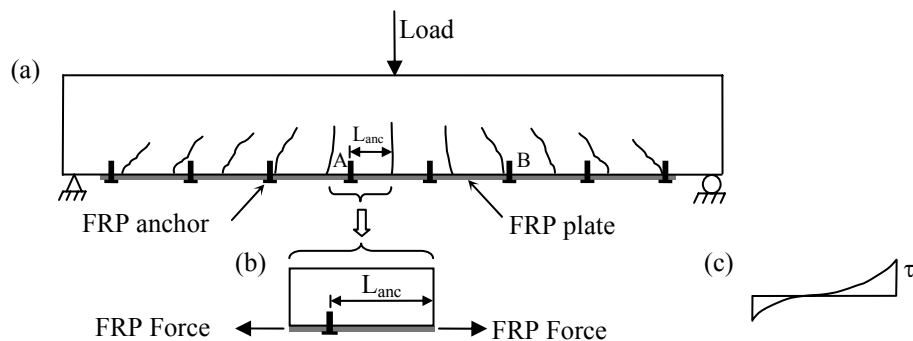


Figure 8. Problem definition: (a) Cracked and anchored FRP-strengthened RC beam, (b) Idealised FRP-concrete joint with anchor, and (c) Idealised elastic interfacial shear stress distribution (pre-debonding)

Tests on the behaviour of FRP anchors in shear have been undertaken on joint scenario shown at the top of Figure 9. Also shown in Figure 9 is the theoretical distribution of strain along the length of the unanchored FRP plate at increasing load levels based upon Yuan et al.'s (2004) solutions. Many permutations of geometrical and material properties of the FRP anchor, FRP plate and concrete can be tested. Inspection of the scenario presented in Figure 8a reveals that the position of the anchor is important and hence a good starting point. Figure 8 therefore shows the positions of three different FRP anchor locations. As the anchor is located closer to the loaded end of the plate, the plate strain is increased and the contribution of the anchor is expected to be enhanced.

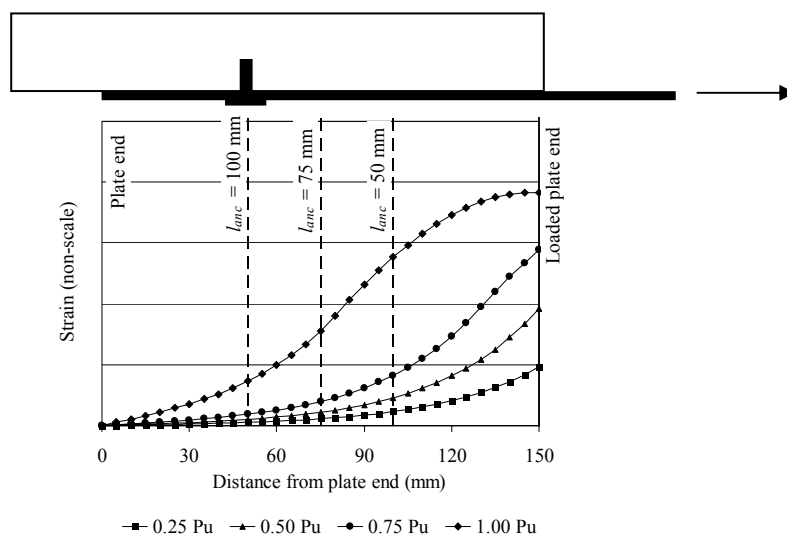


Figure 9. Plate strain distributions

## Experimental Behaviour

The author and his research group have conducted tests on anchored FRP-to-concrete joints under both load and deformation control to date for the scenario presented in Figure 10. In all tests, the anchor fan has been oriented in the direction of load in order to maximise its effectiveness. The variables which have been considered in the load controlled tests have consisted of (i) method of anchor and plate installation (Smith and Kim 2008), (ii) anchor fibre content (Smith and Kim 2008), and (iii) anchor position (Kim and Smith 2009b). In both of these studies, impregnated carbon FRP anchors (Figure 1a) were used. More recent (unpublished) tests have been conducted under deformation controlled loading and these tests have been concerned with optimising the design of the anchor. The variables tested have consisted of (i) all four impregnated and dry carbon and glass FRP anchors shown in Figure 1, and (ii) FRP anchor fibre content.

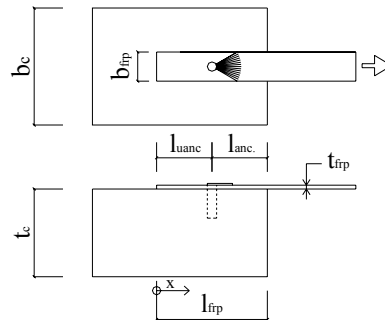
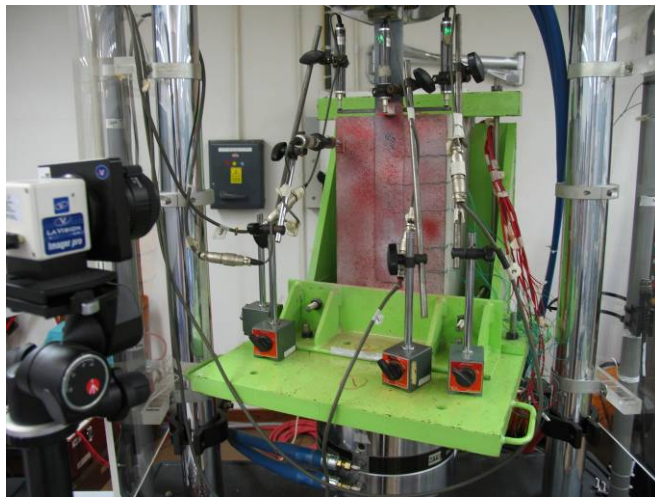


Figure 10. Anchored FRP-to-concrete joint

The set-up for the deformation controlled tests is shown in Figure 11 in which the test specimen is extensively instrumented with linear variable differential transducers (LVDTs) and electric strain gauges. In the foreground on the left in Figure 11a is a high resolution digital camera used to measure FRP and concrete surface strain and deformation fields.



(a) Test set-up



(b) Test in progress (debonded FRP plate evident)

Figure 11. FRP anchored FRP-to-concrete joint shear tests

For the load controlled tests, several failure modes have been observed to date. The FRP anchor was observed to (i) shear off primarily between the concrete and the FRP plate after the FRP plate debonded (Figure 12a), (ii) the anchor fan debonded from the FRP plate after the FRP plate debonded (Figure 12b), and (iii) the FRP anchor dowel pulled out after the FRP plate debonded (Figure 12c). The sequence of FRP plate and FRP anchor failure occurred as (i) debonding of the FRP plate and near simultaneous failure of the anchor (i.e. applicable to the modes in Figures 12a and 12b), and (ii) debonding of the plate well before failure of the FRP anchor (applicable to all three failure modes in Figure 12).

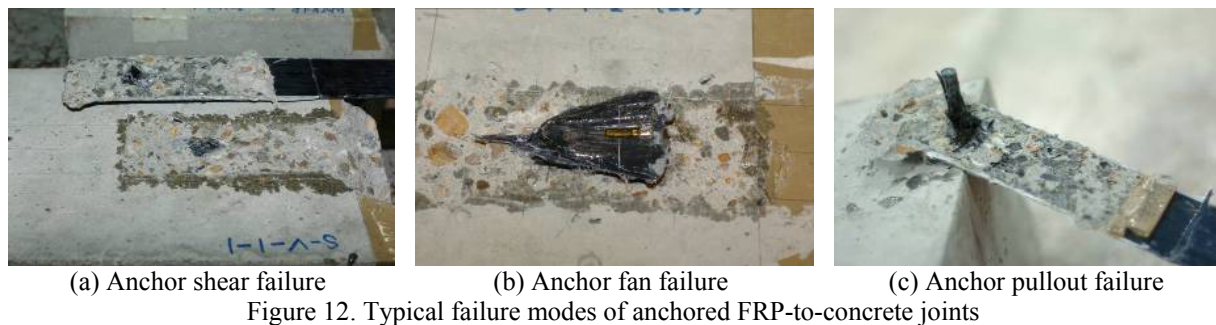


Figure 13 (Kim and Smith 2009b) shows the failure load to decrease the further the anchor is positioned away from the loaded end of the plate for the load controlled tests. This trend is logical considering the plate strain peaks near the loaded plate end (i.e. refer to Figure 9). In addition, the anchors positioned closer to the higher stressed end of the plate were found to be more effective with the average increase in strength over the control specimens for the anchored tests of  $L_{anc} = 50, 75$  and  $100$  mm being 68.7 %, 56.3 % and 18.6 % respectively. It is clear from Figure 13, in which the failure loads of the anchored specimens have been normalised by the average of the three control unanchored tests, that Mode 2B failing specimens provide a lower bound to the joint strength followed by Mode 2A failing specimens.

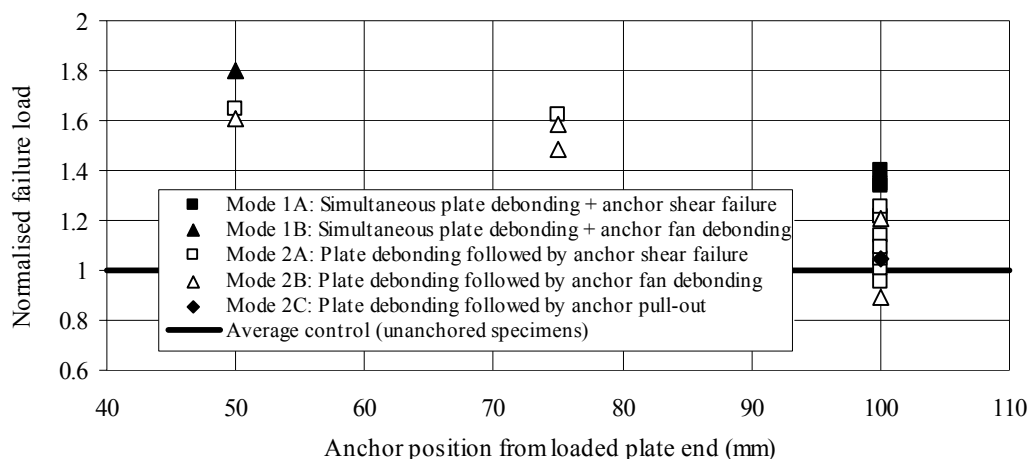


Figure 13. Test summary: Failure load versus anchor distance from unbonded zone

More recently, deformation controlled tests have been conducted by the author and his research group and are hence unpublished to date. In these ongoing tests it has been observed that most of the impregnated anchors failed by shear (Figure 12a), while several of the dry anchors pulled out (e.g. Figure 12c). The benefit of deformation controlled testing has however enabled the post-peak behavior to be captured well as is evident in Figure 9b in which the debonded FRP plate (prior to FRP anchor failure) can be clearly seen. Also, in the deformation controlled tests, none of the anchored joints failed in modes 1A and 2A as described in Figure 13 possibly on account of the energy released during debonding of the FRP plate to be less severe than in the load controlled tests. Figure 14 shows a typical unanchored control joint response in which load versus slip at the loaded end of the FRP plate is plotted. Also shown in this figure is the response of a joint anchored with an impregnated carbon FRP anchor. The geometrical and material properties of the tests are not however given here as they are not deemed important for the exercise; the trends and behaviour are considered more important. A peak load plateau is evident for the control joint result in Figure 14 – this is on account of a long bond length being used (i.e. twice the effective bond length) in addition to deformation controlled loading. For the anchored joint test in Figure 14, the drastic drop in load corresponds to debonding of the FRP plate. Further inspection reveals that the peak force recorded in the anchored joint is approximately 70 % in excess of the control joint and the corresponding slip is approximately eight times greater. This enhancement in joint shear strength is higher than that observed for the load controlled test results presented in Figure 13 possibly on account of the different types of load control. The post-peak reserve of strength in the anchored joint is the contribution of the FRP anchor as well as the friction due to the roughened surface between the debonded FRP plate and the concrete substrate. This significant post-peak reserve of strength, as can also be seen in Figure 14, is approximately equal to the strength of the unanchored joint. The substantial post-peak reserve of slip is also significant (i.e. over 5 mm). Such a post-peak reserve of strength and deformation capacity can offer tremendous ductility benefits to

the overall strengthened system. The anchor eventually failed by shearing in a mode consistent with Figure 12a. Future testing should investigate different material properties and geometrical configurations and optimise the post-peak reserve of strength and slip capacity. Finally, standard tests to determine the strength of FRP anchors should ideally be developed – some progress is being made in this arena by others to date (e.g. Pham et al. 2009)

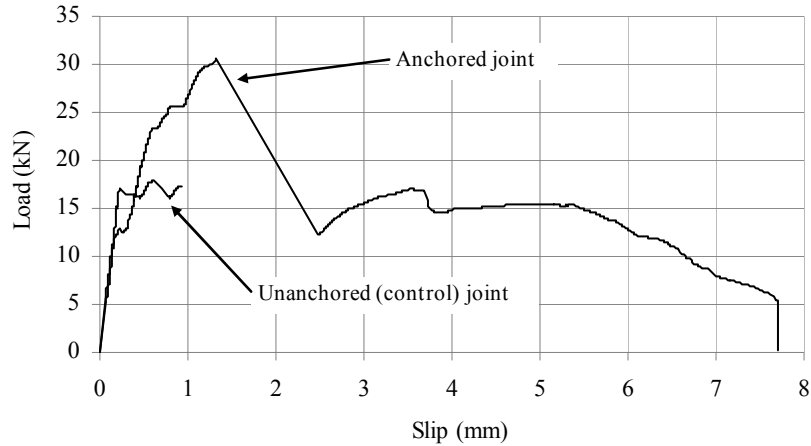


Figure 14. Typical load-displacement responses of unanchored and anchored FRP-to-concrete joints under deformation controlled loading

### Analytical and Numerical Modelling

Kim (2009) derived closed-form analytical solutions for the strength of the joint scenario shown diagrammatically in Figure 10. The solution involved consideration of the fundamental equations of equilibrium and compatibility with a failure criterion described by a fracture mechanics approach. Bond-slip models (e.g. Figure 15) were proposed in order to reflect the elevated fracture energy caused by the anchor (unanchored joint shown shaded in Figure 15). Simplified best-fit and design equations to predict the strength of the joint  $P_u$  are presented as follows. These equations have been calibrated from over 20 load controlled test results to produce a coefficient of variation of approx. 7%. Future research should focus on development of a bond-slip model.

$$P_u = \kappa \beta_w b_{frp} \sqrt{0.616 E_{frp} t_{frp} \sqrt{f_{ct.com}}} \quad (2a)$$

where

$$\kappa = 0.69 + 2.0 e^{-1.75(l_{anc}/l_{frp})} \quad (\text{best-fit model}) \quad (2b)$$

$$\kappa = 0.51 + 2.0 e^{-1.75(l_{anc}/l_{frp})} \quad (\text{design model}) \quad (2c)$$

$$\text{and } f_{ct.com} = 0.395(1.32f_c')^{0.55}, \beta_w = \sqrt{\frac{2 - b_{frp}/b_c}{1 + b_{frp}/b_c}}$$

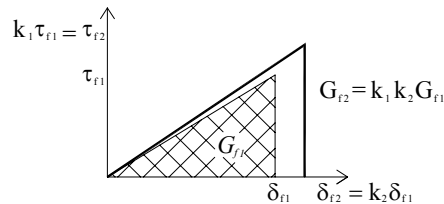


Figure 15. Modified local bond slip model

More recently, progress has been made in the numerical modelling of anchored FRP-to-concrete joints using the applied element method (Mohamed et al. 2009). In this ongoing work, the full response of the assembly has been modelled as well as some of the observed failure modes while the failure load has been predicted with accuracy.

### Design Approach

If we consider again the case of a RC flexural member strengthened with a tension face FRP plate (e.g. Figure 8a), tests have established a distinct tri-linear moment-curvature (or load-deflection) relationship to exist (e.g.

Lam and Teng 2001). When FRP anchors are added to the strengthened member, experimental investigations have found this tri-linear relationship to still hold true (Lam and Teng 2001, Oh and Sim 2004, Ceroni et al. 2008). This tri-linear relationship is also evident in the anchored externally bonded plate result in Figure 1b. In effect, the anchorage is essentially extending the third linear portion of the tri-linear relationship. With this in mind, a design procedure which considers both the strengthening effect of the FRP plate as well as the anchorage provided by the FRP anchor is therefore proposed herein.

The sectional moment of resistance can be calculated using well documented theory which is based on traditional RC theory (e.g. Hollaway and Teng 2008). To consider the effect of premature debonding failure, the maximum usable strain (and stress) with which the FRP plate can resist is limited. This strain is obtained from FRP-to-concrete single joint shear tests results which are then calibrated with strengthened flexural members as was done by Teng et al. (2003) for the case of IC debonding in FRP-strengthened RC beams and slabs. The beneficial effect of FRP anchorage can be incorporated into the analysis by increasing the debonding resistance of the FRP plate.

Figure 16 presents the results of a normalised analytical investigation describing the complete load-deflection response of a FRP-strengthened RC slab using theory presented by Smith and Kim (2009). In this analysis, IC debonding failure has been assumed. The effect of increasing the IC debonding resistance of the FRP strengthening, via the introduction of anchorage, is demonstrated. Anchorage sufficient to achieve a 44 % increase in the IC debonding resistance enables the section to develop its full strength in which failure occurs by rupture of the FRP.

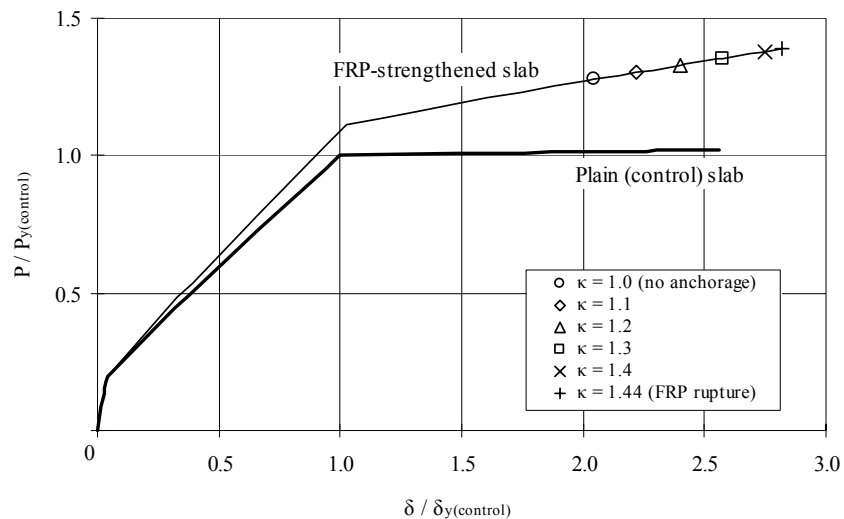


Figure 16. Theoretical load-deflection response for an anchored FRP-strengthened RC slab

In tests on FRP anchored FRP-to-concrete joints, Kim and Smith (2009b) have shown the presence of anchorage to increase the bond strength of unanchored joints by up to 80 %. Future research should concentrate on connecting the model presented in Equation 2 with tests on anchored FRP-strengthened RC flexural members in order to validate the theoretical approach used to generate Figure 16. Design approaches and models which consider anchors applied to other strengthening scenarios can also be left for future research.

## CONCLUSIONS

The rational design of FRP anchors used in the suppression of premature debonding failure modes in FRP strengthened members is the driver for the research presented in this paper. As a result, research on the fundamental behaviour and strength of FRP anchors has been undertaken in addition to the development of analytical models and rational design approaches. Research effort in this field however needs to be maintained in order to advance our knowledge of FRP anchors sufficiently so they can be designed with confidence by design engineers for practical applications.

## ACKNOWLEDGMENTS

Funding provided by the Hong Kong Research Grants Council (General Research Fund Grants HKU 715907E and HKU 716308E) and The University of Hong Kong (HKU Internal Seed Grant) is acknowledged. The author's graduate students, Messrs Seo Jin KIM and Huawen ZHANG, are also gratefully acknowledged.

## REFERENCES

- ACI (2007). *Report on Fiber-Reinforced Polymer (FRP) Reinforcement for Concrete Structures*, ACI 440R-07, American Concrete Institute (ACI), Farmington Hills, MI, USA.
- Aiello, M.A., De Lorenzis, L., Galati, N. and La Tegola, A. (2004). "Bond between FRP laminates and curved concrete substrates with anchoring composite spikes", *Proceedings, Innovative Materials and Technologies for Construction and Restoration, IMTCR 2004*, Lecce, Italy, 6-9 June.
- Ceroni, F., Pecce, M., Matthys, S. and Taerwe, L. (2008). "Debonding strength and anchorage devices for reinforced concrete elements strengthened with FRP sheets", *Composites: Part B*, 39(3), 429-441.
- Cook, R.A., Kunz, J., Fuchs W. and Konz, R.C (1998). "Behavior and design of single adhesive anchors under tensile load in uncracked concrete", *ACI Structural Journal*, 95(1), 9-26.
- Eligehausen, R., Mallee, R. and Silva, J.F. (2006). *Anchorage in Conc. Construction*, Ernst & Young, Germany.
- Hollaway, L.C. and Teng, J.G. (2008). *Strengthening and Rehabilitation of Civil Infrastructures using Fibre-Reinforced Polymer (FRP) Composites*, Woodhead Publishing Limited, Cambridge, UK.
- Kim, S.J. (2008) *Strengthening of Reinforced Concrete Slabs with Penetrations using Unanchored and Anchored Fibre-Reinforced Polymer (FRP) Composites*, Doctor of Philosophy Dissertation, School of Civil and Environmental Engineering, University of Technology Sydney, Australia, under examination.
- Kim, S.J. and Smith, S.T. (2009a). "Behaviour of handmade FRP anchors under tensile load in uncracked concrete", *Advances in Structural Engineering*, APFIS-09 Special Issue, to appear December 2009.
- Kim, S.J. and Smith, S.T. (2009b). "Shear strength and behaviour of FRP spike anchors in cracked concrete", *Proceedings (CD Rom), Ninth International Symposium on Fiber Reinforced Polymer Reinforcement for Concrete Structures, FRPRCS-9*, Sydney, Australia, 13-15 July 2009.
- Kim, S.J. and Smith, S.T. (2009c). "Pullout strength models for FRP anchors in uncracked concrete", under review.
- Lam, L. and Teng, J.G. (2001). "Strength of RC cantilever slabs bonded with GFRP strips", *Journal of Composites for Construction*, ASCE, 5(4), 221-227.
- Mohamed, I., Seracino, R. and Smith, S.T. (2009). "Analysis of FRP-to-concrete joint assemblies with FRP spike anchors using the applied element method", *Proceedings, Second Asia-Pacific Conference on FRP in Structures, APFIS 2009*, Seoul, Korea, 9-11 December.
- Oehlers, D.J. and Seracino, R. (2004). *Design of FRP and Steel Plated RC Structures. Retrofitting Beams and Slabs for Strength, Stiffness and Ductility*, Elsevier, UK.
- Oh, H.-S. and Sim, J. (2004). "Interface debonding failure in beams strengthened with externally bonded GFRP", *Composite Interfaces*, 11(1), 25-42.
- Orton, S.L., Jirsa, J.O. and Bayrak O. (2008). "Design considerations of carbon fibre anchors", *Journal of Composites for Construction*, ASCE, 12(6), 608-616.
- Özdemir, G. (2005) *Mechanical Properties of CFRP Anchorage*, Master of Science Thesis, Middle East Technical University, Turkey.
- Ozbakkaloglu, T. and Saatcioglu, M. (2009). "Tensile behaviour of FRP anchors in concrete", *Journal of Composites for Construction*, ASCE, 13(2), 82-92.
- Pham, L. Jirsa, J.O. and Bayrak O. (2009). "Development of methods for quality control of CFRP anchors", *Proceedings (CD Rom), Ninth International Symposium on Fiber Reinforced Polymer Reinforcement for Concrete Structures, FRPRCS-9*, Sydney, Australia, 13-15 July 2009.
- Smith, S.T. and Teng, J.G. (2002). "FRP-strengthened RC structures. I: Review of debonding strength models", *Engineering Structures*, 24(4), 385-395.
- Smith, S.T. and Kim, S.J. (2008). "Shear strength and behaviour of FRP spike anchors in FRP-to-concrete joint assemblies", *Proceedings (CD ROM), Fifth International Conference on Advanced Composite Materials in Bridges and Structures, ACMBS-V*, Winnipeg, Canada, 22-24 September.
- Smith, S.T. and Kim, S.J. (2009). "Calculation of deflection of FRP-strengthened RC slabs using a tri-linear moment-curvature relationship", *Proceedings, Advanced Composites in Construction Conference, ACIC 2009*, Edinburgh, UK, 1-3 September, 239-249.
- Seliem, H.M., Sumner, E.A., Seracino, R. and Smith, S.T. (2008). "Field testing of RC slabs with openings strengthened with CFRP", *Proceedings (CD Rom), Fourth International Conference on FRP Composites in Civil Engineering, CICE 2008*, Zürich, Switzerland, 22-24 July.
- Tan, K.H. and Patoary, M.K.H. (2004). "Strengthening of masonry walls against out-of-plane load using fiber-reinforced polymer reinforcement", *Journal of Composites for Construction*, ASCE, 8(1), 79-87.
- Teng, J.G., Smith, S.T., Yao, J. and Chen, J.F. (2003). "Intermediate crack induced debonding in RC beams and slabs", *Construction and Building Materials*, 17(6-7), 447-462.
- Teng, J.G., Yuan, H. and Chen, J.F. (2006). "FRP-to-concrete interfaces between two adjacent cracks: Theoretical model for debonding failure", *International Journal of Solids and Structures*, 43, 5750-5778.
- Yuan, H., Teng, J.G., Seracino, R., Wu, Z.S. and Yao, J. (2004). "Full-range behaviour of FRP-to-concrete bonded joints", *Engineering Structures*, 26(5), 553-565.